

# Energy Analysis of a Combined Cycle Organic Rankine Cycle / Vapor compression Refrigeration Investigation of Organic Fluids

M.Tech. Scholar Vaibhav Vivek<sup>1</sup> Prof. Sujeet Kumar Singh<sup>2</sup>

Department of Mechanical  
EngineeringPCST, Bhopal MP India.

## Abstract

In this study, the energy and energy analysis of a combined cycle was carried out. This cycle consists of an organic Rankine cycle and a vapor compression refrigeration cycle for producing the cooling effect. Four organic fluids were used as working fluids such as R600a, R245fa, RC318 and R236fa. The parametric analysis allowed us to characterize the combined system and to study the effect of some parameters that were used to estimate the thermal and energy efficiency of the studied system. The results showed that the operating parameters have a significant impact on the performance of the combined system. Due to environmental issues of R600a is recommended as a superior candidate for the ORC-VCR system for retrieving low-grade thermal energy. On the other hand, the results of the energy destruction distribution showed also that maximum energy destruction rate is found in R600a and minimum is in RC318.

**Keywords:** Rankine cycle, refrigeration, energy, organic fluids.

## I. INTRODUCTION

Nowadays, there are numerous attempts in the utilization of renewable energies such as geothermal heat, wind energy, and solar energy as clean energy sources for electricity production or cooling processes. Also, waste heat can be considered as renewable and clean energy, since it is free energy and there is no direct carbon emission.

Waste heat can be rejected at a wide range of temperatures depending on the industrial processes [1]. An ejector refrigeration system and an absorption refrigeration system can be activated by thermal energy source with a temperature range from 100 to 200 °C. They have several advantages such as simple structure, reliability, low investment cost, slight maintenance, long lifetime, and low running cost [2, 3]. Nevertheless, they are not appropriate for thermal sources less than 90 °C and are also not appropriate for working in high-temperature surroundings. Furthermore, the minimum cooling temperature could be achieved by both systems is 5 °C [4]. The

Working fluid selection has a large influence on the performance of combined organic Rankine cycle-vapor compression refrigeration (ORC-VCR) system. Several studies have been done on the working fluid selection, i.e. R12, R22, R113, and R114 for the ORC-VCR system and identified the most suitable one, which may yield highest coefficient of performance (COP) [8–13]. The refrigerants R123, R134a, and R245ca were evaluated to find the best one for the ORCVCR system by Aphornratana and Sriveerakul [14].

The results indicated that R123 achieves the best system performance. An ORC-VCR system activated by a low temperature source utilizes R134a was analyzed by Kim and Perez-Blanco [4]. The minimum cooling temperature could be achieved by the system was -10 °C. An ORC-VCR system utilizing two different candidates for the power and refrigeration cycles, i.e. R245fa and R134a, respectively was investigated by Wang et al. [1]. The system coefficient of performance (COPS) attained approximately 0.5. Six candidates, namely R134a, R123, R245fa, R290, R600a, and R600, were

investigated to determine appropriate working fluid for ORC-VCR system by Bu et al. [15]. They concluded that R600a is the most suitable candidate. A combined ORC with a vehicle air conditioning system using R245fa, R134a, pentane, and cyclopentane as working fluids was studied by Yue et al. [16]. Their results indicated that R134a gives the maximum economic and thermal performance. An ORCVCR system powered by low-grade thermal energy using two different substances for the power and refrigeration cycles was studied by Mole's et al. [17].

They concluded that the best candidates for the power and refrigeration cycles are R1336mzz (Z) and R1234ze (E), respectively. From the aforementioned introduction, it is clear that there is still a need for screening of alternative candidates for ORCVCR system. The present study concentrates on the production of electricity or cooling from low-temperature renewable energies such as waste heat or geothermal heat having a temperature around 100 °C. The potential use of RC318, R236fa, R600a and R245fa as working fluids in the ORC-VCR system is assessed. The performance of the system is characterized by the COPS and system efficiency.

## II. DESCRIPTION OF THE INTEGRATED ORC-VCR SYSTEM

This subsystem consists of a pump, an ORC Evaporator, a Turbine, and condenser (Figure 1). In the ORC evaporator, the working fluid is initially heated and then vaporized at ORC evaporation temperature  $T_{eva}$  by means of the heat absorbed from the heat source  $Q_{ORC}$ . Then the steam generated at high pressure enters the expander, whose enthalpy is converted into power.

Then, the fluid enters the condenser, where it condenses at condensation temperature  $T_{cond}$  due to the rejection of  $Q_{cond}$  to the external medium, which is at temperature  $T_0$ . Next, the working fluid enters the pump, which moves the fluid to the ORC Evaporator to complete the cycle [17]. The net mechanical power provided by the ORC cycle is used to drive the compressor of the VCR cycle. This second subsystem consists of a compressor, a condenser, Expansion valves, and VCREvaporator (Figure 1). In the VCR Evaporator, the working fluid absorbs the cooling load  $Q_{eva\_VCR}$  from the cooling space at the VCR evaporation temperature

$T_{evap\_VCR}$ . Then, the working fluid is compressed in the compressor, and in the condenser, the working fluid rejects  $Q_{cond}$  at  $T_{cond}$  to the condensing medium which is  $T_0$ . Finally, it expands in the Expansion valve.

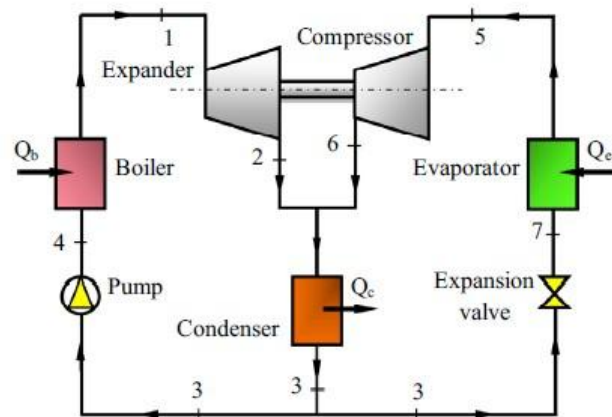


Figure 1: ORC-VCR system schematic diagram.

The selection of working fluid for the ORC-VCR systems is a critical issue, where it plays a key role in the system performance. An appropriate working fluid should achieve both minimal environmental issues and high system performance. Because of their zero ozone depletion potential (ODP), HFCs and FCs have been considered as working fluids substituting hydro chlorofluorocarbons (HCFCs) and chlorofluorocarbons (CFCs) in VCR cycle, ORC, ejector refrigeration cycle and integrated cycles [2,22]. Recently, these fluids are regulated due to their high global warming potential (GWP). Consequently, research is still ongoing for other fluids, which may have lower environmental issues.

Using HCs as alternative working fluids is one possibility. HCs have a very low GWP, environmentally friendly and superior thermophysical properties [23]. The only controversy issue against using HCs is its flammability. However, the flammability will not constitute the biggest challenge in utilizing HCs with appropriate safety precautions. Also, HFEs have been proposed as alternative working fluids due to their zero ODP and significantly low GWP. HFEs have other environmental features such as shorter atmospheric lifetime (ALT) and lower GWP as compared with HFCs. Also, they are non-flammable and low toxicity [24]. Furthermore, numerous HFOs with low environmental impact are proposed as working fluids [2,12].

### III. MATHEMATICAL MODEL AND COMPUTATIONAL PROCEDURE

The thermodynamic mathematical model for the ORC-VCR system illustrated in Fig. 1 is described as follows: With respect to the ORC:

$$W_{exp} = m_{ORC}(h_1 - h_{2a}) = m_{ORC}(h_1 - h_{2s})\eta_{exp}$$

where  $W_{exp}$  is the output power from the expander during process (1-2a) in kW,  $m_{ORC}$  is the mass flow rate of the working fluid in the ORC in kg/s,  $h_1$  is the expander inlet specific enthalpy in kJ/kg,  $h_{2a}$  is the expander exit actual specific enthalpy in kJ/kg,  $h_{2s}$  is the expander exit isentropic specific enthalpy in kJ/kg, and  $\eta_{exp}$  is the expander isentropic efficiency.

$$W_{exp} = m_{ORC}(h_{4a} - h_3) = m_{ORC}(h_{4s} - h_3)/\eta_{pump}$$

where,  $WP$  is the inlet power to the pump during process (3-4a) in kW,  $h_{4a}$  is the pump exit actual specific enthalpy in kJ/kg,  $h_3$  is the pump inlet specific enthalpy in kJ/kg,  $h_{4s}$  is the isentropic specific enthalpy at the pump outlet in kJ/kg, and  $\eta_p$  is the pump isentropic efficiency.

$W_{net} = W_{exp} - WP$  where,  $W_{net}$  is the net output power from the ORC in kW

$$Q_b = m_{ORC}(h_1 - h_{4a})$$

where,  $Q_b$  is the heat transfer rate to the working fluid in the boiler during the process (4a-1) in kW,  $h_1$  is the boiler outlet specific enthalpy in kJ/kg, and  $h_{4a}$  is the boiler inlet actual specific enthalpy in kJ/kg.

$$\eta_{ORC} = W_{net}/Q_b$$

where,  $\eta_{ORC}$  is the organic Rankine cycle efficiency.

With respect to the VCR cycle:

$$Q_e = m_{VCR}(h_5 - h_7)$$

where,  $Q_e$  is the rate of heat transfer to the working fluid in the evaporator during process (7-5) in kW,  $m_{VCR}$  is the mass flow rate of the working fluid in the VCR in kg/s,  $h_5$  is the evaporator outlet specific enthalpy in kJ/kg, and  $h_7$  is the evaporator inlet specific enthalpy in kJ/kg.

$$W_c = m_{VCR}(h_5 - h_{6a}) = m_{VCR}(h_5 - h_{6s})/\eta_c$$

where,  $W_c$  is the inlet power to the compressor during process (5-6a) in kW,  $h_5$  is the compressor inlet specific enthalpy in kJ/kg,  $h_{6a}$  is the compressor outlet actual specific enthalpy in kJ/kg,  $h_{6s}$  is the compressor outlet isentropic specific enthalpy in kJ/kg, and  $\eta_c$  is the compressor isentropic efficiency.

$$W_c = W_{net}$$

The VCR cycle COP is defined as follows:

$$COP_{VCR} = Q_e/W_c$$

The COPs can be calculated as follows:

$$COPs = \eta_{ORC} COP_{VCR}$$

The compressor compression ratio (CMR) during the process (5-6a) and the expander expansion ratio (EPR) during the process (1-2a) are measures for the required compressor and expander sizes, respectively, and described as follows:

$$CMR = P_{6a}/P_5$$

$$EPR = v_{2a}/v_1$$

The basic values of the ORC-VCR system operating parameters and their ranges are presented in Table 1. EES code was established to assess the ORC-VCR system performance as well as the CMR and EPR with various candidates under different working conditions.

**Table - I:** The basic values of the parameters utilized in the ORC-VCR system and their ranges

Parameter	Touaibi et. al. (2018)	Present
Mass flow rate of the working fluid in ORC	1 Kg/s	-
Isentropic efficiency of the feed pump	85%	-
Boiler temperature	80°C	60-105 °C
Isentropic efficiency of the expander	80%	-
Condenser temperature	40°C	30-55 °C
Evaporator temperature	80°C	-15 to 15 °C
Isentropic efficiency of the compressor	85%	-

### IV. RESULTS AND DISCUSSION

In this work, the performance of ORC-VCR system using four refrigerants, i.e. RC318, R236fa, R600a and R245fa as working fluids was calculated and analyzed.

#### 1. EES Code Validation

To validate the present model, the simulation results have been compared with the available numerical data in the literature using the R600a as working fluid. The results of this study were compared with the simulation data published by Touaibi (2018). Table 4.1 presents the combined system performances for the same operating conditions used by Touaibi (2018). According to comparison, the

agreement between the two simulation results is good.

**Table 2:** Validation of the model with the results of the Touaibi (2018)

Parameter	Touaibi (2018)	Present
$\eta_{ORC}$	0.0789	0.0971
$COP_{VCR}$	5.12	7.518
$\eta_s$	0.49	0.725
$COP_s$	0.40	0.73

**Table -3:** Performances of the combined system ORC-VCR according to the studied working fluids

Parameter	R600a	RC318	R245fa	R236fa
$\eta_s$	0.6654	0.5445	0.6798	0.6464
$COP_s$	0.73	0.6144	0.7458	0.7107
CMR	2.192	1.522	2.88	2.403
EPR	3.538	6.859	4.299	4.459

The results in Table 3 show that among all candidates, R600 and R245fa with the highest critical temperatures have the maximum and the same COPS values, whereas RC318, R1234yf, and R1270 with the lowest critical temperatures have the minimum COPS values.

## 2. Influence of Boiler Temperature on the System Performance

The effect of boiler temperature on the ORC-VCR system performance with different candidates, are presented in below figures.

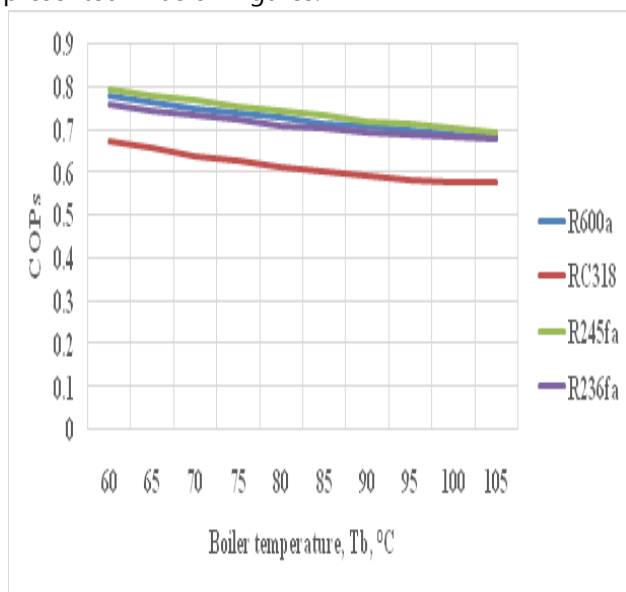


**Figure 2:** The effect of boiler temperature on the COPS for various candidates in the basic ORC-VCR system.

Fig. 2 displays the alteration in COPS as a function of the boiler temperature for different candidates in the

basic ORC-VCR system. This figure shows that the COPS of the system decreases as the boiler temperature increases for all candidates. Among the proposed working fluids, R245fa achieve the highest COPS for all boiler temperatures, while RC318, R600a, and R236fa attain the lowest COPS.

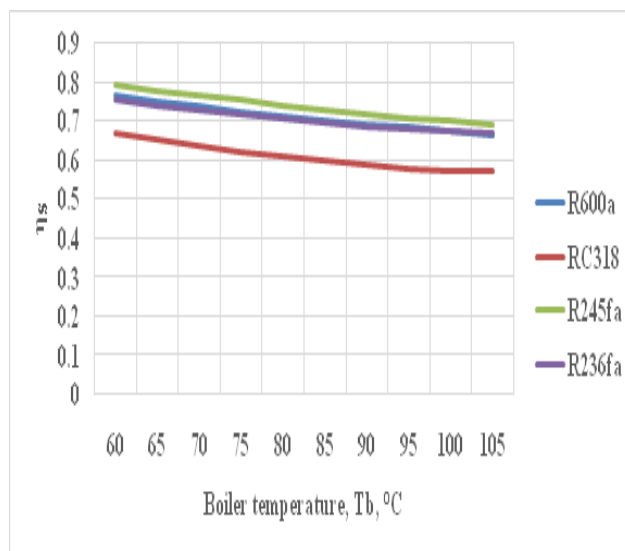


**Figure 3:** The effect of boiler temperature on the system efficiency for various candidates in the basic ORC-VCR system.

The variation of  $\eta_{sys}$  as a function of  $T_b$  for all candidates in the typical system is displayed in Fig. 3. As can be observed from the figure, the increase of  $T_b$  leads to a decrease in system efficiency,  $\eta_{sys}$ . Among the proposed working fluids, R245fa achieve the highest system efficiency for all boiler temperatures, while RC318 attain the lowest system efficiency.

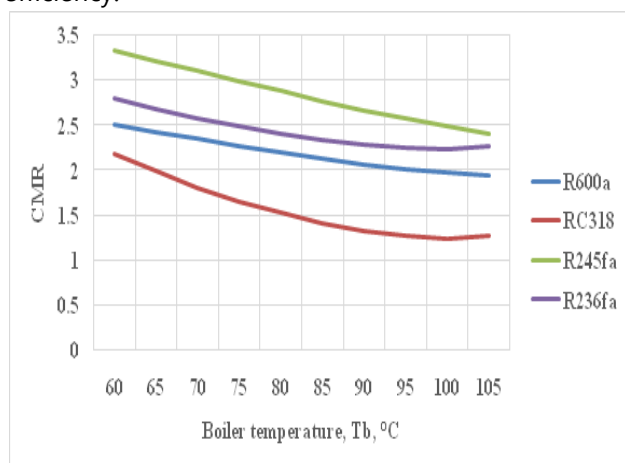


**Figure 4:** The effect of boiler temperature on the CMR for various candidates in the basic ORC-VCR system.

Fig. 4 exhibits the change in CMR values as a function of the boiler temperature for different candidates in the basic ORC-VCR system. This figure shows that the CMR decreases as the boiler temperature increases for all candidates. This is due to the rise of saturation pressure with the temperature. The CMR values at a boiler temperature of 90°C are nearly twice those at 60 °C for all candidates.

The maximum CMR is achieved by R245fa. The minimum CMR is attained by RC318, R600a and R236fa. Fig. 5 exhibits the change in EPR values as a function of the boiler temperature for different candidates in the basic ORC-VCR system. This figure shows that the EPR increases as the boiler temperature increases for all candidates. This is due to the rise of saturation pressure with the temperature. The EPR values at a boiler temperature of 90°C are nearly twice those at 60 °C for all candidates. The maximum EPR is achieved by RC318fa. The minimum EPR is attained by R245fa, R600a and R236fa.

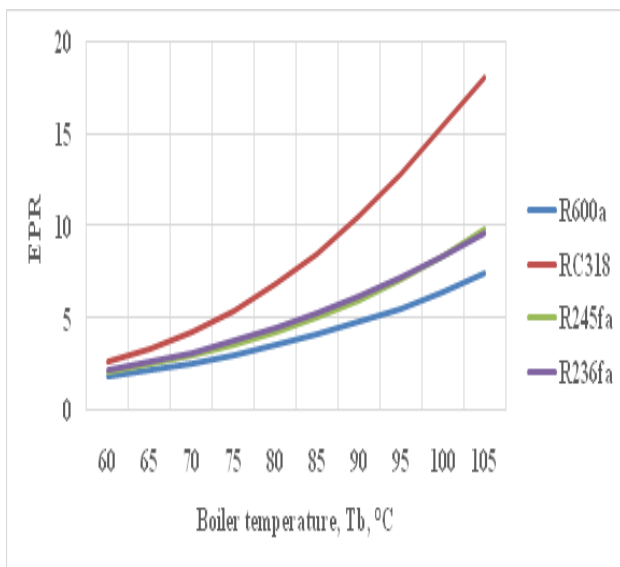


**Figure 5:** The effect of boiler temperature on the EPR for various candidates in the basic ORC-VCR system.

### 3. Influence of Condenser Temperature on the System Performance.

The variation of COPS with the condenser temperature for all candidates in the basic ORC-VCR system is illustrated in Fig. 6-9.

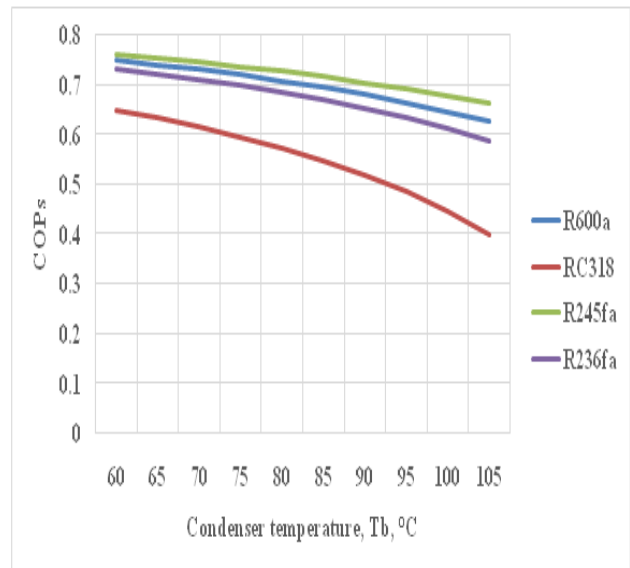


**Figure 7:** The effect of condenser temperature on the COPS for various candidates in the basic ORC-VCR system.

It is observed from the figure that, the condenser temperature has a large effect on the COPS. This is because the condenser temperature has an effect on both VCR cycle and ORC individually. The rejected heat is governed by condenser temperature, which is an additional parameter to boost the cycle efficiency in addition to the boiler temperature. Small values of rejected heat are preferable to achieve high efficiencies in both cycles. It can be noticed from Fig. 7 that the COPS reduces with the increase in condenser temperature for all candidates.

This is justified by the truth that as the temperature and pressure kept constant at the inlet of the compressor, the increase in condenser temperature causes the rise of pressure and enthalpy at the compressor exit. Among the proposed working fluids, R245fa achieve the highest COPS values for all condenser temperatures, while RC318 attains the lowest COPS. The variation of system efficiency with the condenser temperature for various candidates in the basic ORC-VCR system is displayed in Fig. 8. Generally, the increase in condenser temperature leads to decrease of system efficiency for all candidates. RC318 attained the lowest system efficiency, while the highest was achieved by R245fa for all condenser temperatures.

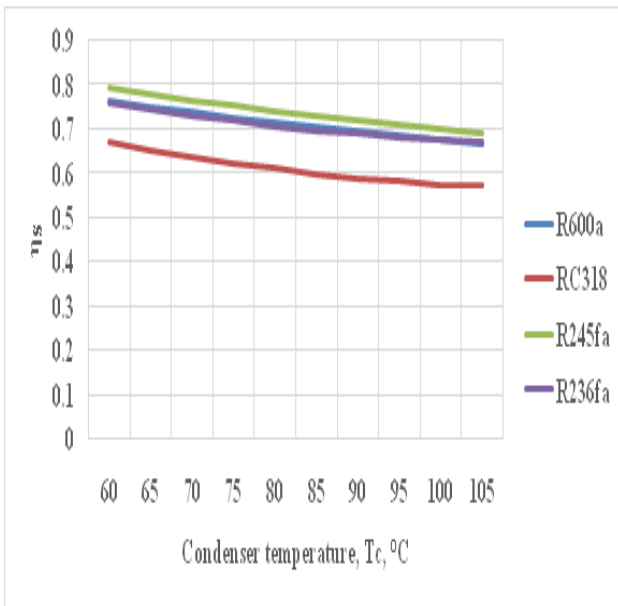


**Figure 8:** The effect of condenser temperature on the system efficiency for various candidates in the basic ORC-VCR system.

working fluids are smaller at low than that at high condenser temperatures.

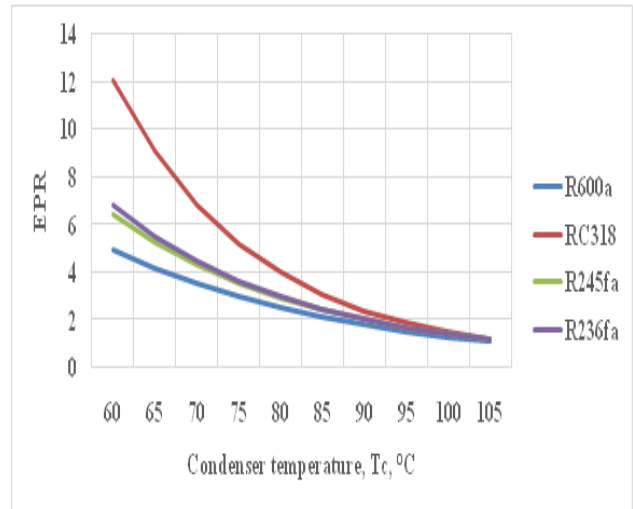


**Figure 10:** The effect of condenser temperature on the EPR for various candidates in the basic ORC-VCR system.

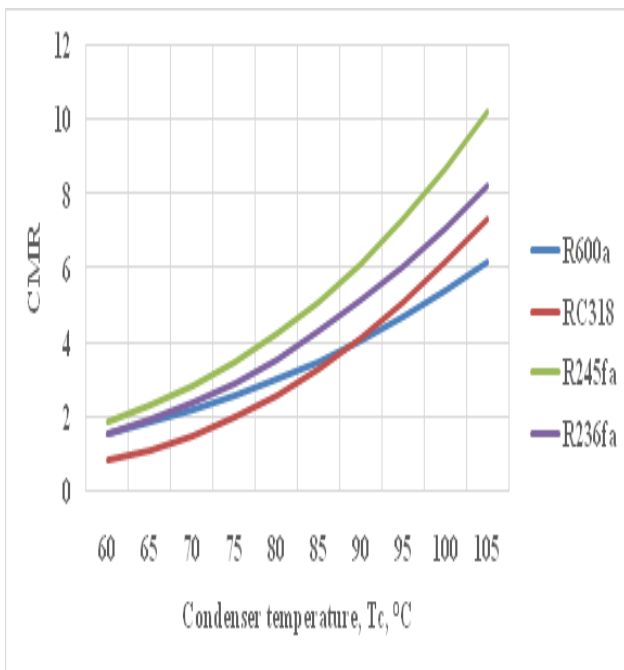


**Figure 9:** The effect of condenser temperature on the CMR for various candidates in the basic ORC-VCR system.

The influences of condenser temperature on the CMR for different working fluids in ORC-VCR system are illustrated in Fig. 9, respectively. It is detected from these figures that with the increase in condenser temperature, the CMR increases. This is logically when taking into account the thermos-physical properties effect of these candidates. The variations between the CMR values for the proposed

The influences of condenser temperature on the EPR for different working fluids in ORC-VCR system are illustrated in Fig. 10, respectively. It is detected from these figures that with the increase in condenser temperature, the EPR decreases. This is logically when taking into account the thermos-physical properties effect of these candidates. The variations between the EPR values for the proposed working fluids are smaller at high than that at low condenser temperatures.

#### 4. Influence of Evaporator Temperature on the System Performance

The variation of COPS with the condenser temperature for all candidates in the basic ORC-VCR system is illustrated in below Figures.

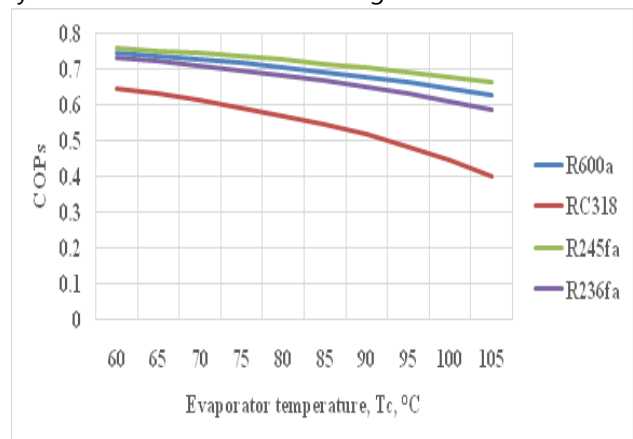


**Figure 11:** The effect of evaporator temperature on the COPS for various candidates in the basic ORC-VCR system.

It can be noticed from Fig. 11 that, the increment in evaporator temperature leads to decrement of the COPS. This can be interpreted by the truth that with the increase in evaporator temperature its saturation pressure decreases. Among the proposed candidates, R245fa attain the highest COPs values, while R600, RC318 and R236fa has the lowest COPs values for all evaporator temperatures.

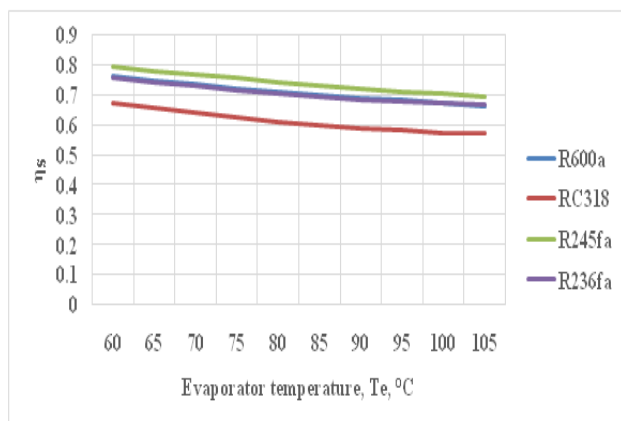


**Figure 12:** The effect of evaporator temperature on the system efficiency for various candidates in the basic ORC-VCR system.

It can be noticed from Fig. 12 that, the increment in evaporator temperature leads to decrement of the system efficiency. This can be interpreted by the truth that with the increase in evaporator temperature its saturation pressure decreases. Among the proposed candidates, R245fa attain the highest system efficiency values, while R600, RC318 and R236fa has the lowest system efficiency values for all evaporator temperatures.

The variation of CPR as a function of  $T_{eva}$  for all candidates in the typical system is presented in Fig. 13. The general trend in the figure is an increase of CMR with the increase of  $T_{eva}$ . This is because of the evaporator pressure decreases as  $T_{eva}$  rises, which leads to an increase in CMR at constant  $T_c$ . The increase in CMR leads to a decline in the required  $\dot{W}_{comp}$  which results in a decrease in CPOs. Accordingly, from the energetic viewpoint, to get maximum COPs the CMR should be minimum. Among all candidates, R245fa attains the maximum CMR values while RC318 achieves the minimum values for all studied  $T_{eva}$ .

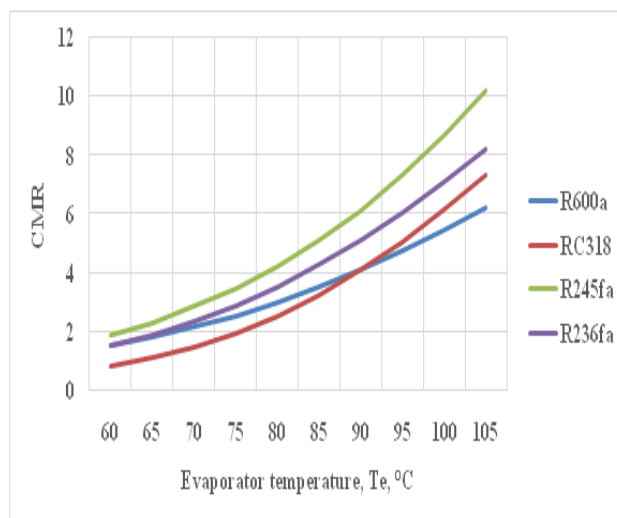


**Figure 13:** The effect of evaporator temperature on the CMR for various candidates in the basic ORC-VCR system.

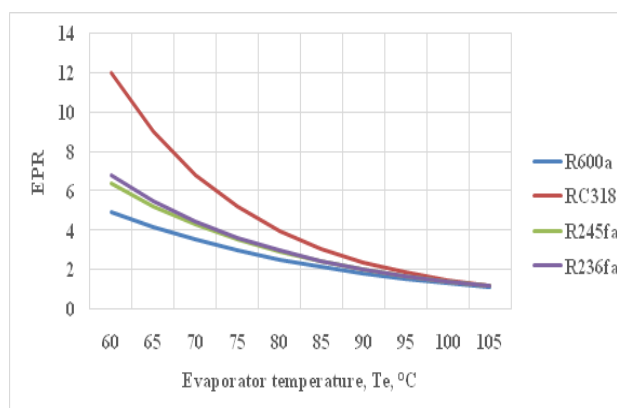


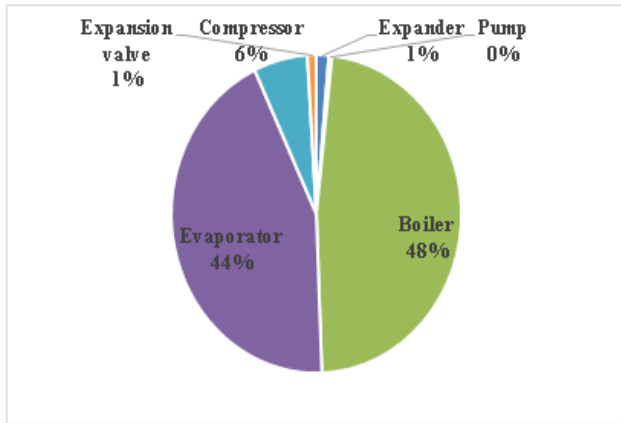
**Figure 14:** The effect of evaporator temperature on the EPR for various candidates in the basic ORC-VCR system.

The variation of EPR as a function of  $T_{eva}$  for all candidates in the typical system is presented in Fig. 14. The general trend in the figure is a decline of EPR with the increase of  $T_{eva}$ . This is because of the evaporator pressure increases as  $T_{eva}$  rises, which leads to a decrease in EPR at constant  $T_c$ . The decrease in EPR leads to a decline in the required  $\dot{W}_{comp}$  which results in an increase in CPOs. Among all candidates, RC318 attains the maximum EPR values while R600a achieves the minimum values for all studied  $T_{eva}$ .

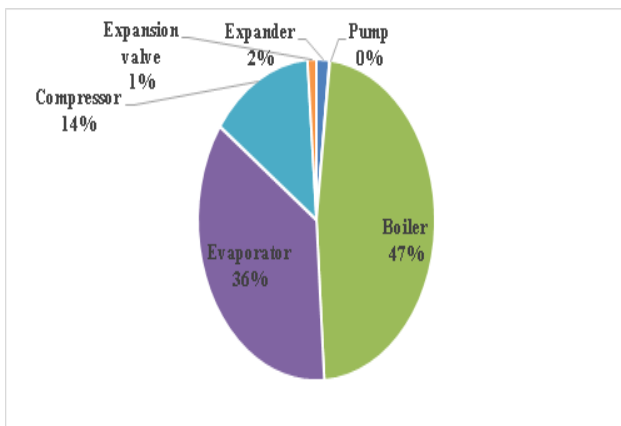
### 5. Energy Destruction Distribution in the Combined System ORC-VCR

The energy destruction ratio is a beneficial parameter for comparison of energy destruction among different system components and to determine the weak points of a system. The total destroyed energy

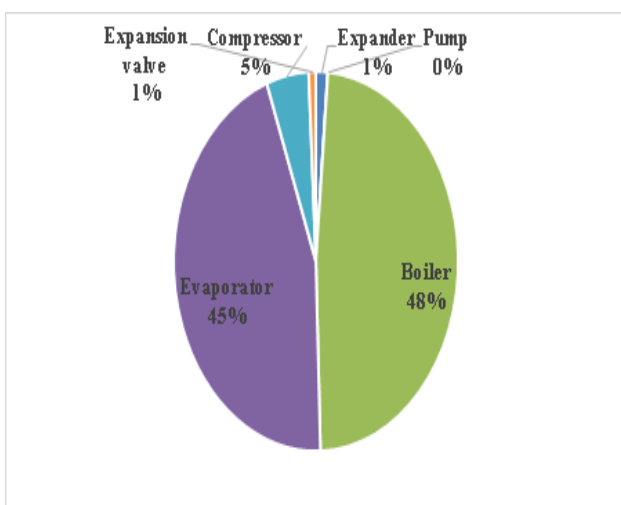
rate is 578.3 kW (R600a), 201.5 kW (RC318), 340.3 (R245fa) and 261.8 (R236fa). By comparing the energy destruction proportion for each component of the system, it is clear that the largest amount of destroyed energy occurs in the boiler.



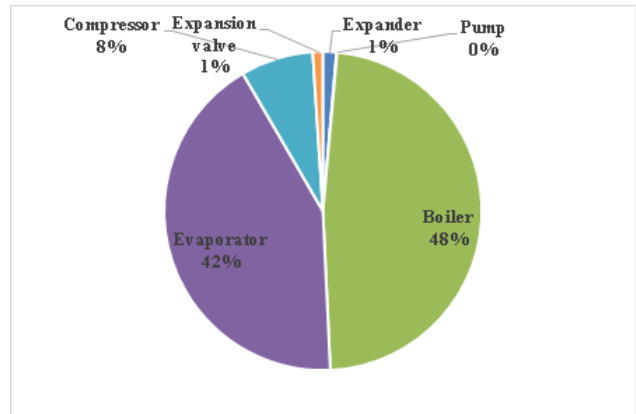
(a) R600a



(a) RC318



(c) R245fa



(d) R236fa

**Figure 15:** Energy destruction distribution in the system according to the studied working fluids.

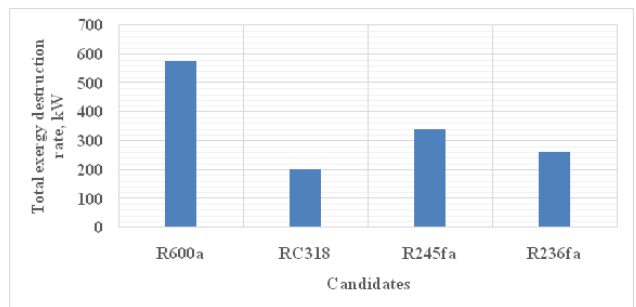


**Figure 16:** Total energy destruction rate in the system according to the studied working fluids.

It is cleared the maximum total energy destruction rate is found in R600a and minimum is in RC318.

## V. CONCLUSION

In the present research, the performance of ORC-VCR system activated by low-grade thermal energy is investigated. Some common refrigerants such as RC318, R236fa, R600a and R245fa are proposed as working fluids. The effects of evaporator, condenser, and boiler temperatures on the ORC-VCR system performance are also examined and discussed.

1. The results indicate that all studied parameters have comparable influences on the ORC-VCR system performance for all candidates. In detail, as the evaporator, condenser and boiler temperatures increase, the COPs decreases for all candidates.
2. Also, as the evaporator, condenser and boiler temperatures increase, the system efficiency decreases for all candidates.
3. Also, as the evaporator and boiler temperatures increase, the compression ratio increases and the



expansion ratio increases, respectively, while the reverse occurs with the condenser temperature.

4. From the acquired results it can be concluded that, among all candidates, R600a achieve the highest COPs values.
5. The distribution of energy destruction shows that for the four studied fluids, most of the energy is destroyed at the boiler followed by at the ORC evaporator and condenser.
6. The energy destruction ratio is a beneficial parameter for comparison of energy destruction among different system components and to determine the weak points of a system. The total destroyed energy rate is 578.3 kW (R600a), 201.5 kW (RC318), 340.3 (R245fa) and 261.8 (R236fa).
7. Due to environmental issues of R600a is recommended as a superior candidate for the ORC-VCR system for retrieving low-grade thermal energy.

## REFERENCES

- [1]. Javanshir, N., Seyed Mahmoudi, S. M., & Rosen, M. A. (2019). Thermodynamic and Exergoeconomic Analyses of a Novel Combined Cycle Comprised of Vapor-Compression Refrigeration and Organic Rankine Cycles. *Sustainability*, 11(12), 3374.
- [2]. Salim, M. S., & Kim, M. H. (2020). Multi-objective thermo-economic optimization of a combined organic Rankine cycle and vapour compression refrigeration cycle. *Energy Conversion and Management*, 199, 112054.
- [3]. Saleh, B., Aly, A. A., Alogla, A. F., Aljuaid, A. M., Alharthi, M. M., Ahmed, K. I., & Hamed, Y. S. (2021). Performance investigation of organic Rankine-vapor compression refrigeration integrated system activated by renewable energy. *Mechanics & Industry*, 20(2), 206.
- [4]. Kutlu, C., Erdinc, M. T., Li, J., Wang, Y., & Su, Y. (2019). A study on heat storage sizing and flow control for a domestic scale solar-powered organic Rankine cycle-vapour compression refrigeration system. *Renewable Energy*, 143, 301-312.
- [5]. Liang, Y., Yu, Z., & Li, W. (2020). A Waste Heat-Driven Cooling System Based on Combined Organic Rankine and Vapour Compression Refrigeration Cycles. *Applied Sciences*, 9(20), 4242.
- [6]. Saleh, B. (2018). Energy and exergy analysis of an integrated organic Rankine cycle-vapor compression refrigeration system. *Applied Thermal Engineering*, 141, 697-710.
- [7]. Kaşka, Ö., Yılmaz, C., Bor, O., & Tokgöz, N. (2018). The performance assessment of a combined organic Rankine-vapor compression refrigeration cycle aided hydrogen liquefaction. *International Journal of Hydrogen Energy*, 43(44), 20192-20202.
- [8]. Sag, N. B. Analysis of a Combined Organic Rankine Cycle and Vapor Compression Refrigeration Cycle.
- [9]. Touaibi, R., Köten, H., Feidt, M., & Boydak, O. Investigation of three Organic Fluids Effects on Exergy Analysis of a Combined Cycle: Organic Rankine Cycle/Vapor Compression Refrigeration.
- [10]. Toujani, N., Bouaziz, N., Chrigui, M., & Kairouani, L. (2018). Performance analysis of a new combined organic Rankine cycle and vapor compression cycle for power and refrigeration cogeneration. *Transactions of the Institute of Fluid-Flow Machinery*.
- [11]. Asim, M., Leung, M. K., Shan, Z., Li, Y., Leung, D. Y., & Ni, M. (2017). Thermodynamic and thermo-economic analysis of integrated organic Rankine cycle for waste heat recovery from vapor compression refrigeration cycle. *Energy Procedia*, 143, 192-198.
- [12]. Bounefour, O., & Ouadha, A. (2017). Performance improvement of combined organic Rankine-vapor compression cycle using serial cascade evaporation in the organic cycle. *Energy Procedia*, 139, 248-253.
- [13]. Ahmed, Z., & Mahanta, D. K. Thermodynamic Analysis of Combined ORC-VCR Powered by Waste Energy from Diesel Engine. *System*, 14, 15.
- [14]. He, W. F., Ji, C., Han, D., Wu, Y. K., Huang, L., & Zhang, X. K. (2017). Performance analysis of the mechanical vapor compression desalination system driven by an organic Rankine cycle. *Energy*, 141, 1177-1186.
- [15]. Patel, B., Desai, N. B., & Kachhwaha, S. S. (2017). Thermo-economic analysis of solar-biomass organic Rankine cycle powered cascaded vapor compression-absorption system. *Solar Energy*, 157, 920-933.
- [16]. Nasir, M. T., & Kim, K. C. (2016). Working fluids selection and parametric optimization of an Organic Rankine Cycle coupled Vapor Compression Cycle (ORC-VCC) for air conditioning using low grade heat. *Energy and Buildings*, 129, 378-395.
- [17]. Bu, X., Wang, L., & Li, H. (2013). Performance analysis and working fluid selection for

geothermal energy-powered organic Rankine-vapor compression air conditioning. *Geothermal Energy*, 1(1), 2.

- [18]. Bounefour, O., & Ouadha, A. (2014, November). Thermodynamic analysis and working fluid optimization of a combined ORC-VCC system using waste heat from a marine diesel engine. In *ASME 2014 International Mechanical Engineering Congress and Exposition* (pp. V06AT07A084-V06AT07A084). American Society of Mechanical Engineers.
- [19]. Bu, X., Wang, L., & Li, H. (2021). Working fluids selection for fishing boats waste heat powered organic Rankine-vapor compression ice maker. *Heat and mass transfer*, 50(10), 1479-1485.
- [20]. Nasir, M. T., & Kim, K. C. (2015). Energetic and Exergetic Evaluation of Various Combination of Working Fluids in Dual Fluid Organic Rankine Cycle Powered Vapor Compression Cycle.
- [21]. K.S. Rawat, H. Khulve, A.K. Pratihar.(2020). Thermodynamic Analysis of Combined ORC-VCR System Using Low Grade Thermal Energy. *International Journal for Research in Applied Science & Engineering Technology (IJRASET)*.
- [22]. Molés, F., Navarro-Esbrí, J., Peris, B., Mota-Babiloni, A., & Kontomaris, K. K. (2015). Thermodynamic analysis of a combined organic Rankine cycle and vapor compression cycle system activated with low temperature heat sources using low GWP fluids. *Applied Thermal Engineering*, 87, 444-453.
- [23]. Sethi, A., Becerra, E. V., & Motta, S. Y. (2016). Low GWP R134a replacements for small refrigeration (plug-in) applications. *International journal of refrigeration*, 66, 64-72.
- [24]. Kim, K. H., & Perez-Blanco, H. (2015). Performance analysis of a combined organic Rankine cycle and vapor compression cycle for power and refrigeration cogeneration. *Applied Thermal Engineering*, 91, 964-974.
- [25]. Yilmaz, A. (2019). Transcritical organic Rankine vapor compression refrigeration system for intercity bus air-conditioning using engine exhaust heat. *Energy*, 82, 1047-1056.